IEEE Access
Multidisciplinary | Rapid Review | Open Access Journal

Received April 10, 2020, accepted May 11, 2020, date of publication May 18, 2020, date of current version June 1, 2020.

Digital Object Identifier 10.1109/ACCESS.2020.2995260

Risk-Based Performance of Combined Heat and Power Based Microgrid Using Information Gap Decision Theory

SAYYAD NOJAVAN[1] **AND KITTISAK JERMSITTIPARSERT**[2]
[1]Department of Electrical Engineering, University of Bonab, Bonab 5551761167, Iran
[2]Social Research Institute, Chulalongkorn University, Bangkok 10330, Thailand

Corresponding author: Kittisak Jermsittiparsert (kittisak.j@chula.ac.th)

ABSTRACT In this paper, to get optimal scheduling of microgrids (MGs) in short-term, info-gap decision-theory (IGDT) is applied to assess load uncertainty. In order to provide a comprehensive load uncertainty study, best and worst possible conditions are evaluated using IGDT's functions of opportunity and robustness, respectively, in which risk-taker and risk-averse strategies are obtained while deterministic case study is also carried-out under the risk-neutral strategy. Real-time pricing (RTP) and time-of-use pricing (TOU) of demand response program (DRP) are applied to peak-load management. For each strategy, three cases as without DRP, TOU-DRP, and RTP-DRP are investigated. According to the results in the risk-neutral strategy, by applying TOU-DRP and RTP-DRP, operating cost is reduced about 2.5% and 6.6%, respectively. In the risk-averse strategy, by considering MG operating cost equal to \$6,000, the MG will robust against load uncertainty up to 18.37%, 21.52%, and 24.82% for without DRP, TOU-DRP, and RTP-DRP cases, respectively. In the risk-taker strategy, MG operating cost for 28% of load reduction, operating costs will be equal to \$3,698.12, \$3,605.21, and \$3,338.87 for without DRP, TOU-DRP, and RTP-DRP, respectively, in comparison with the risk-neutral strategy.

INDEX TERMS Information gap decision theory, load uncertainty, heat and power micro-grid, flexible load management, robustness and opportunity function.

I. INTRODUCTION

Today, due to depletion of fossil fuels and environmental issues, power systems experience significant changes [1]. Demand response programs (DRPs) and high penetration of renewable energy sources are most important experienced changes [2]. Microgrids (MGs) can be considered as a key part to supply load in the presence of mentioned changes. MGs broadly are divided into AC, DC and hybrid MG according to power frequency [3], [4] which can increase penetration of renewable generation and provide reliable and economic power supply [5]. Utilization of MGs faces different issues because of managing multiple generating resources and loads [6]. Maintaining the equilibrium between loads and generation of the MG and power exchange between the upstream grid and other MGs are the most challenging issues [7]. As a result, efficient energy management is vital to utilize multiple benefits of MGs [8].

The associate editor coordinating the review of this manuscript and approving it for publication was Saeid Nahavandi.

A. LITERATURE REVIEW

Based on their operating frequency, MGs can be broadly categorized into three sub-section as DC, AC and hybrid MGs. Optimal operation of MGs has addressed by researchers [9]–[11]. In [12], optimal planning of MGs is evaluated using a stochastic programming framework presented for 24-h period. Minimizing the total operation cost a MG is investigated in [13]. In the presence of electric vehicles (EVs), internal sources of a typical MG are surveyed in [14]. MGs operation under high uncertainty of RESs is evaluated in [15] through developing two-stage model of stochastic programming method. A generalized formulation for energy management of an MG which is combined with Artificial intelligence techniques is proposed in [16]. By taking cost and emission into account, multi-objective functions are defined to get optimal dispatch of MG's generating units [17], [18]. In order to get optimal solution for the MG's economic-dispatch problem (EDP), four different methods containing particle swarm optimization, direct search method (DSM), lambda logic and lambda iteration have been used in [19].

In order to increase economical and operational efficiencies of an MG, CHP resources which generates simultaneously power and heat energies, can be integrated into the power systems [20]. EDP of CHP based MG, through taking dependency of heat and power, is analyzed in [21], [22]. The unit-commitment (UC) and EDP of MG's units examined by using improved mixed-integer linear-programming (MILP) approach in [23]. Ref. [24] has studied energy management of MG to decrease operation cost and reduce emissions while the use of RESs is increased. The genetic algorithm is applied to determine optimal discharging and charging of energy storage unit in an MG in order to effectively deal with the multi-objective functions in [25].

DRPs can also be used in MG scheduling problem as an effective tool to decrease operating cost. US Department of Energy has defined DRPs as changes in end-user clients' electric consumption patterns to response the changes of electricity price or to promote the consumers to reduce the compensations under reliability problems of the system [26]. The operation strategy and pricing of an MG retailer in the presence of DRP are studied in [27]. DRP's contribution to the optimal integration of RESs such as wind power (WT), biomass, wind power, small hydro, CHP and photovoltaic (PV) plants is presented in [28].

B. NEW CONCEPTS AND CONTRIBUTIONS

In this paper, optimal operation of a CHP-based MG is evaluated by considering load uncertainty under DRPs such as RTP and TOU. To increase the MG efficiency, heat and power dispatch is investigated simultaneously. Different generation unit as CHP, power-only unit, heat only unit and storage is considered to satisfy power and heat demands. Also, IGDT is proposed to consider load uncertainty. Modeling of the various uncertainty statuses are considered by using IGDT-technique's functions of robustness and opportunity. Deterministic results without considering load uncertainty are presented as the risk-neutral strategy. Finally, robust and opportunity results are investigated as the risk-averse and risk-taker strategies, respectively.

C. PAPER ORGANIZATION

The reminder of this paper is organized as: MG and DRP models are described in Section II. IGDT-technique is introduced and applied to the model in sections III and IV, respectively. The risk-neutral, risk-taker results, and risk-averse results are presented in Section V. Lastly, this work is concluded in Section VI.

II. PROBLEM FORMULATION

The MG model contains ESS, heat only (HO), power only (PO) unit, heat buffer tank, and two CHP units. DRPs are considered to flat the load profile and reduce demand at high price times which will result reduction in operating cost.

A. OBJECTIVE FUNCTION AND POWER BALANCE

The objective function of the system is developed based on total operating cost of the MG, including purchased power from the power market, heat and power generation costs, ESS degradation cost minus revenue of power injection the upstream-grid. Equation (1) describes the objective function.

$$OF = \sum_{h=1}^{24} \left\{ \begin{array}{l} \lambda_h \times P_h^{G,buy} + \sum_{i=1}^{N_{CHP}} C(P_{i,h}^{CHP}, H_{i,h}^{CHP}) \\ +C(\mathrm{P}_h^{PO}) + C(\mathrm{H}_h^{PO}) \\ + \sum_{j\in CHP,\mathrm{PO,b}} (C_{j,SU}.SU_h^j + C_{j,SD}.SD_h^j) \\ +C_k^{\deg}(\sum_{k=1}^{N_k} \frac{P_{k,h}^{disc}}{\eta_k^{disc}} + \eta_k^C \times P_{k,h}^C) - \lambda_h \times P_h^{G,sell} \end{array} \right\} \quad (1)$$

where λ_h, is the power price in ($/MWh), $P_h^{G,sell}$ and $P_h^{G,buy}$ present purchased/sold electricity power from/to the market (MWh), $C(P_{i,h}^{CHP}, H_{i,h}^{CHP})$, $C(\mathrm{P}_h^{PO})$, and $C(\mathrm{H}_h^{PO})$ are the cost functions of CHP, PO and HO units, respectively. The shut-down and startup costs of generation plants presented in $ by using $C_{j,SD}$ and $C_{j,SU}$, respectively; SD_h^j/SU_h^j is binary variables of shut-down/start-up status for each unit at time h, $C_k^{\deg}$ is the battery degradation cost in $/MWh, and $P_{k,h}^C/P_{k,h}^{disc}$ is charged/discharged power of the ESS in MW.

At each time step, sum of generated power and acquired power from the upstream-grid minus the total load of MG after implementation of DRPs should be equal to zero which is modeled by Eq. (2).

$$P_h^{G,buy} - P_h^{G,\mathrm{sell}} + \sum_{i=1}^{N_{CHP}} P_{i,h}^{CHP} + P_h^{PO} + P_h^{disc} - P_h^C - P_h^{DR} = 0 \quad (2)$$

where P_h^{DR}, is the electric load profile after implementing DRP.

B. MODELING OF CHP UNITS

Two different feasible operating regions (FORs), as shown in Fig. 1, are considered for each of the CHP units in the MG. As discussed in [12], the heat and electric generations in CHP units are related to each other. Equations (3)-(21) models first type of CHP-units [23].

$$P_{i,\mathrm{h}}^{CHP} - P_{i,\mathrm{A}}^{CHP} - \frac{P_{i,\mathrm{A}}^{CHP} - P_{i,\mathrm{B}}^{CHP}}{H_{i,\mathrm{A}}^{CHP} - H_{i,\mathrm{B}}^{CHP}}(H_{i,\mathrm{h}}^{CHP} - H_{i,\mathrm{A}}^{CHP}) \le 0 \quad (3)$$

$$P_{i,\mathrm{h}}^{CHP} - P_{i,B}^{CHP} - \frac{P_{i,B}^{CHP} - P_{i,C}^{CHP}}{H_{i,B}^{CHP} - H_{i,C}^{CHP}}(H_{i,\mathrm{h}}^{CHP} - H_{i,B}^{CHP}) \ge -(1 - \mathrm{V}_{i,h}^{CHP}) \times M \quad (4)$$

$$P_{i,\mathrm{h}}^{CHP} - P_{i,C}^{CHP} - \frac{P_{i,C}^{CHP} - P_{i,\mathrm{D}}^{CHP}}{H_{i,\mathrm{C}}^{CHP} - H_{i,\mathrm{D}}^{CHP}}(H_{i,\mathrm{h}}^{CHP} - H_{i,\mathrm{C}}^{CHP}) \ge -(1 - \mathrm{V}_{i,h}^{CHP}) \times M \quad (5)$$

$$0 \le P_{i,h}^{CHP} \le P_{i,A}^{CHP} \times V_{i,h}^{CHP} \quad (6)$$

$$0 \le H_{i,h}^{CHP} \le H_{i,B}^{CHP} \times V_{i,h}^{CHP} \quad (7)$$

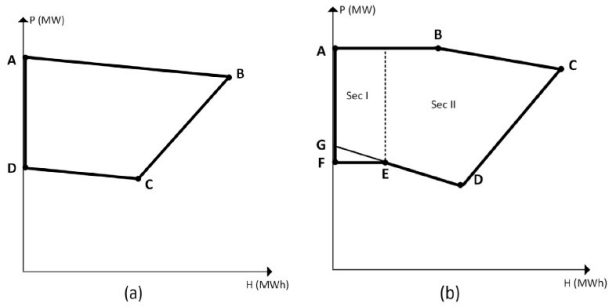

FIGURE 1. CHP-units' FOR. (a) Type 1. (b) Type 2.

where, $P_{i,h}^{CHP}$ is generated electric power of each CHP in MW at time h, $H_{i,h}^{CHP}$ is generated heat of each CHP in MWth, A, B, C, and D are marginal points of feasible operating of each CHP units type, $V_{i,h}^{CHP}$ is binary variable for presenting the status of commitment of each CHP unit and M is a large enough number. Note that each area of FOR in Fig. 1 is described by one of the Eqs. (3)-(7). The area below the AB is formulated by Eq. (3). Equations (4) and (5) describe the upper part of the curve BC and CD, respectively. The output power will be zero when binary variable $V_{i,h}^{CHP}$ is zero. This issue is presented by Eq. (4) and Eq. (5). Equations (6) and (7) show the limits of power and heat generation, respectively.

The second type FOR of the CHP unit is modeled by Eq. (8)-(16) based on [29]. To apply model, the second type of the FOR with conventional formulation, the area FEG is ignored. So, $X_{1,h}$ and $X_{2,h}$, which are binary variables, are considered to divide the discussed area into two sub-sections as sub section I and II.

$$P_{i,\mathrm{h}}^{CHP} - P_{i,B}^{CHP} - \frac{P_{i,B}^{CHP} - P_{i,C}^{CHP}}{H_{i,B}^{CHP} - H_{i,C}^{CHP}}(H_{i,\mathrm{h}}^{CHP} - H_{i,B}^{CHP}) \le 0 \quad (8)$$

$$P_{i,\mathrm{h}}^{CHP} - P_{i,C}^{CHP} - \frac{P_{i,C}^{CHP} - P_{i,D}^{CHP}}{H_{i,C}^{CHP} - H_{i,D}^{CHP}}(H_{i,\mathrm{h}}^{CHP} - H_{i,C}^{CHP}) \le 0 \quad (9)$$

$$P_{i,\mathrm{h}}^{CHP} - P_{i,\mathrm{E}}^{CHP} - \frac{P_{i,\mathrm{E}}^{CHP} - P_{i,\mathrm{F}}^{CHP}}{H_{i,\mathrm{E}}^{CHP} - H_{i,\mathrm{F}}^{CHP}}(H_{i,\mathrm{h}}^{CHP} - H_{i,\mathrm{E}}^{CHP}) \ge -(1 - X_{1,h}) \times M \quad (10)$$

$$P_{i,\mathrm{h}}^{CHP} - P_{i,D}^{CHP} - \frac{P_{i,D}^{CHP} - P_{i,E}^{CHP}}{H_{i,\mathrm{D}}^{CHP} - H_{i,\mathrm{E}}^{CHP}}(H_{i,\mathrm{h}}^{CHP} - H_{i,D}^{CHP}) \ge -(1 - X_{2,h}) \times M \quad (11)$$

$$0 \le H_{i,h}^{CHP} \le H_{i,C}^{CHP} \times V_{i,h}^{CHP} \quad (12)$$

$$0 \le P_{i,h}^{CHP} \le P_{i,A}^{CHP} \times V_{i,\mathrm{h}}^{CHP} \quad (13)$$

$$X_{1,h} + X_{2,h} = V_{i,h}^{CHP} \quad (14)$$

$$H_{i,h}^{CHP} - H_{i,E}^{CHP} \le (1 - X_{1,h}) \times M \quad (15)$$

$$H_{i,h}^{CHP} - H_{i,E}^{CHP} \le -(1 - X_{2,h}) \times M \quad (16)$$

where, E and F determine the FOR of the second CHP unit type as shown in Fig. 1. Operation states of CHP units are presented by $X_{1,h}$ and $X_{2,h}$ for the first or second convex section of the FOR.

In abovementioned equations, the area under the curve BC, upper the curve CD, over the DE and EF curves are modeled by Eqs. (8)-(11), respectively. The generation of power and heat energies of the CHP are limited by Eq. (12) and Eq. (13), respectively. Equation (14) is used to select operation area of the CHP as discussed earlier.

Total cost of CHP's operation is modeled by Eq. (17) as presented in [30].

$$\begin{aligned} &C(P_h^{CHP}, H_h^{CHP}) \\ &\quad = \mathrm{a} \times (P_h^{CHP})^2 + b \times P_h^{CHP} + c + d \times (H_h^{CHP})^2 \\ &\qquad + e \times H_h^{CHP} + f \times H_h^{CHP} \times P_h^{CHP} \end{aligned} \quad (17)$$

where a, b, c, d, and f are coefficients of the CHP's cost function.

C. MODELING OF POWER-ONLY AND HEAT-ONLY UNITS

Related constraints to the operation of heat and power only units are presented by Eqs. (18)-(19), respectively.

$$H_h^{b-\min} \times V_h^b \le H_h^b \le H_h^{b-\max} \times V_h^b \quad (18)$$

$$P_h^{PO-\min} \times V_h^{PO} \le P_h^{PO} \le P_h^{PO-\max} \times V_h^{PO} \quad (19)$$

where P_h^{PO} is the power output of power only unit in MW, $P_h^{PO-\max}/P_h^{PO-\min}$ is the maximum/minimum output constraints of the power only unit,$H_h^{b-\max}$ and $H_h^{b-\min}$ are the maximum and minimum heat limits of the boiler, H_h^b is the heat generation of the boiler unit at time h (MWth).

Equations (20) and (21) describe the cost functions of PO and HO units.

$$C(P_h^{PO}) = \lambda_{PO} \times P_h^{PO} \quad (20)$$

$$C(H_h^b) = \lambda_b \times H_h^b \quad (21)$$

where $C(P_h^{PO})$ is the power only unit's cost function, $C(H_h^b)$ is cost-function of the boiler and λ_{PO} is PO unit's power price in \$/MW h. Finally, λ_b is the boiler's power price in \$/MWth.

D. MODELING OF ESS

Equations (22)-(23) models the Charged and discharged constraints of the ESS.

$$\begin{aligned} 0 \le P_h^c \le b_h^c \times P_h^{c,\max}, \\ 0 \le P_h^{disc} \le b_h^{disc} \times P_h^{disc,\max} \end{aligned} \quad (22)$$

$$E_k^{\min} \le E_{h,s} \le E_k^{\max} \quad (23)$$

where b_h^c/b_h^{disc} is the charging/discharging states' binary variable, $E_{h,s}$ is the ESS' capacity in kWh, $E_k^{\max}/E_k^{\min}$ is maximum/minimum stored energy in ESS in kWh. Simultaneous discharging and charging of the battery can be restricted by Eq. (24).

$$b_h^c + b_h^{disc} \le 1; \quad b_h^c, \mathrm{b}_h^{disc} \in \{1, 0\} \quad (24)$$

Finally, by using Eq. (25) the stored energy in the ESS at each time step can be calculated.

$$E_{h+1} = E_h + (\eta^c \times P_h^c - \frac{P_h^{disc}}{\eta^{disc}}) \quad (25)$$

E. E MODELING OF HEAT BUFFER TANK

The total stored heat in heat buffer tank can be calculated using Eq. (26). The heat buffer-tank has been utilized to store heat energy which is described by Eq. (26) [31].

$$\bar{H}_h = \sum_{i=1}^{N_{CHP}} H_{i,h}^{CHP} + H_h^b \tag{26}$$

By using β_{gain} /β_{loss} which is excess/loss heat generation of the CHP unit in the shutdown/startup time, heat losses can be modeled as Eq. (27).

$$H_h = \bar{H}_h - \beta_{loss}.SU_h^i + \beta_{gain}.SD_h^i; \quad \forall i \in CHP, b \tag{27}$$

At each period, the Eq. (28) is used to calculated the available heat capacity in the heat buffer.

$$B_h = (1-\eta) \times B_{h-1} + H_h - \bar{H}_h^{load} \tag{28}$$

where η, is heat loss rate of the buffer tank.

The maximum available capacity of heat storage is limited by using Eq. (29).

$$B_{\min} \le B_h \le B_{\max} \tag{29}$$

where $B_{\max}/B_{\min}$ is maximum/minimum capacity of the heat buffer tank in MW.

The ramping down and ramping-up rates of heat-storage device, Eqs. (30) and (31) are used, respectively.

$$B_h - B_{h-1} \le B_{\max}^{ch\arg e} \tag{30}$$
$$B_{h-1} - B_h \le B_{\max}^{disch\arg e} \tag{31}$$

where, $B_{\max}^{disch\arg e}/B_{\max}^{ch\arg e}$ is the maximum rate of discharging/charging of the heat buffer tank.

F. SHUT-DOWN AND START-UP STATUSES

Using Eqs. (32) and (33), the start-up and shut-down status of each unit can be modeled.

$$SU_h^i = V_h^i \times (1 - V_{h-1}^i), \quad \forall i \in CHP, PO, b \tag{32}$$
$$SD_h^i = (1 - V_h^i) \times V_{h-1}^i, \quad \forall i \in CHP, PO, b \tag{33}$$

G. MODELING OF DRP

In the current power systems, the concept of DRP are considered as feasible and reliable tool to provide various service from peak-shaving to ancillary services. Generally, DRPs are grouped as time-based and incentive based. The time-based (price based) DRPs shift load from an expensive period to an inexpensive period which provides many advantages such as avoiding costly energy procurement and unnecessary capacity expansion [32]. To get mentioned benefits of the DRP, RTP and TOU rates of DRPs are used to evaluate their impact on the final results.

1) MODELING OF TOU RATE OF DRP

Eq. (34) models the TOU rate of DRP [33].

$$P_h^{DR} = P_h^D + ldr_h \tag{34}$$

where ldr_h is transferred load from one load level to load level of h.th hour. ldr_h is calculated through Eq. (35).

$$ldr_h = DR_h \times P_h^D \tag{35}$$

where DR_h is the contribution coefficient of DRP and P_h^D is the initial demand in MWh. It is assumed that sum of shifted load during the time period is equal to zero which is stated by Eq. (36).

$$\sum_{h=1}^{24} ldr_h = 0 \tag{36}$$

At each time-step, DR_h is limited by Eq. (37).

$$DR_h^{\min} \le DR_h \le DR_h^{\max} \tag{37}$$

In this paper $DR_h^{\min}$ is assumed to be equal -30% and $DR_h^{\max}$ to be equal $+30\%$.

2) MODELING OF RTP RATE OF DRP

The RTP model is developed via the forecasted data for load profile of the system which is expressed in Eq. (38).

$$T_d = \sum_{h=1}^{24} P_h^D \tag{38}$$

where T_d is the total load of the MG. The mean load demand, P_{av}, is calculated by Eq. (39).

$$P_{av} = \frac{T_d}{24} \tag{39}$$

Using the calculated mean load demand, Eq. (40) is used to get float factor of RTP.

$$\gamma_h = \frac{P_h^D}{P_{av}} \tag{40}$$

The RTP model can be expressed as follows:

$$\lambda_{RTP} = \gamma_h.\lambda_{TOU} \tag{41}$$
$$\lambda_{RTP}^{Min} \le \lambda_{RTP} \le \lambda_{RTP}^{Max} \tag{42}$$

where λ_{TOU} is the benchmark-price, which, in this paper, considered to be equal to the TOU pricing. $\lambda_{RTP}^{Min}/\lambda_{RTP}^{Max}$ is the minimum/maximum limits of the RTP.

With taking the RTP of DRP into account, new load profile of the MG can be formulated as Eq. (43).

$$P_h^{DR} = P_h^D + \frac{E.P_h^D(\lambda_{RTP} - \lambda_{TOU})}{\lambda_{RTP}} \tag{43}$$

where E is the elasticity coefficient of demand-price. It should be denoted that E is taken according to the historical load information and customer types. Based on [30], E can get any value between -0.5 and 0 which in this paper, is assumed equal to -0.5.

III. IGDT TECHNIQUE

In the power system, there are many important parameters such as power price and load demand with uncertainty [34]. The uncertainty in the power systems may have desirable or undesirable effects on the system. To model desired and undesired aspects of uncertainty of any parameter, the IGDT method offers two functions as opportunity and robustness, respectively. System model, operation requirements, and uncertainty modeling are the three parts of IGDT which is will be detailed in the following sections.

A. SYSTEM MODELING

Output or input structure of under study system is presented in the system modeling section which is referred to as $C(p, \zeta)$. In system model, ζ is called uncertainty parameter and p is considered as the decision variable. In the problem of optimal scheduling MG, total operating cost is the system model and load demand is the uncertainty parameter.

B. OPERATION REQUIREMENTS

The expected performance of the under study system, MG in this case, in different circumstances is described in operation requirements. The functions of robustness and opportunity are used to analyze these expectations. Therefore, the robustness and opportunity functions of MG will be as follow:

$$\hat{\alpha}(C_r) = \max_{\alpha} \{\alpha : \max(C(p, \zeta)) \leq C_r\} \quad (44)$$

$$\hat{\beta}(C_o) = \min_{\alpha} \{\alpha : \min(C(p, \zeta)) \leq C_o\} \quad (45)$$

where C_r and C_o are the critical costs of robustness function and opportunity functions, respectively. As shown in Eq. (44), MG is resistant to increasing load demand, with considering the risk-averse strategy. $\hat{\alpha}$ is degree of resistance against increasing load demand which means the higher values for $\hat{\alpha}$ is preferable.

MG will benefit from the load reduction modeled through function of opportunity of the IGDT as expressed in Eq. (45), under risk-taker strategy. As $\hat{\beta}$ states the lowest amount of load reduction, the lower values for $\hat{\beta}$ is preferable. Note $\hat{\beta}$ is the lowest value of α. In addition, the operating cost of MG should be less than a fixed value, C_o.

C. UNCERTAINTY MODELING

In order to model the uncertainty parameter (ζ), fractional-error model of the IGDT technique can be used. This model is established in next section.

IV. PROPOSED IGDT-BASED RISK-CONSTRAINED FORMULATION

In the following sub-sections, IGDT-technique is implemented to deal with load uncertainty in MG's total operating cost optimization.

A. UNCERTAINTY MODELING

The uncertainty parameter, which is the load demand in this study, as said before, is modeled using the info-gap model which provided in Eq. (46).

$$U(\alpha, \tilde{P}_h^{DR}) = \left\{ P_h^{DR} : \frac{\left| P_h^{DR} - \tilde{P}_h^{DR} \right|}{\tilde{P}_h^{DR}} \leq \alpha \right\}, \quad \alpha \geq 0 \quad (46)$$

where P_h^{DR} is the load demand after applying DRPs.

B. ROBUSTNESS FUNCTION

The $\hat{\alpha}(C_r)$ parameter in the robustness function of the IGDT determines the maximum resistance versus the uncertainty of load. The goal of robust performance of the MG is desire to select the risk-averse strategy by paying more money [35]. Robustness function of IGDT-technique is simulated as:

$$\hat{\alpha}(C_r) = \max \left\{ \alpha : \left(\max \cos t^{total} \leq C_r = (1+\omega) C_b \right) \right\} \quad (47)$$

where, $\hat{\alpha}(C_r)$ is the robustness function. In risk averse strategy, with satisfying all requirements of the MG, the parameter of the uncertainty is maximized.

$$\hat{\alpha}(C_r) = \max \alpha \quad (48)$$

$$Subject\ to : Max\{OF\} \leq C_r \quad (49)$$

$$(1-\alpha)\tilde{P}_h^{DR} \leq P_h^{DR} \leq (1+\alpha)\tilde{P}_h^{DR} \quad (50)$$

$$\text{Eqs. } (2) - (43) \quad (51)$$

Eq. (52) will be considered to get the maximum increase of the uncertainty parameter in which the maximum objective function is obtained.

$$P_h^{DR} = (1+\alpha)\tilde{P}_h^{DR} \quad (52)$$

Therefore, in the risk-averse strategy, the robustness function will be shortened as:

$$\hat{\alpha}(C_r) = \max \alpha \quad (53)$$

$$Subject\ to : \ OF \leq C_r \quad (54)$$

$$P_h^{DR} = (1+\alpha)\tilde{P}_h^{DR} \quad (55)$$

$$\text{Eqs.}(2) - (43) \quad (56)$$

C. OPPORTUNITY FUNCTION

The opportunity function models any downsizing in uncertain parameter that will result possible increase in benefit. The Opportunity function of IGDT is as:

$$\hat{\beta}(C_o) = \min \left\{ \alpha : (\min \cos t^{total} \leq C_o) = (1-\Upsilon) C_b \right\} \quad (57)$$

Maximizing the benefits of reduction in the uncertainty parameter with meeting MG's requirements is the main goal of the IGDT-technique.

$$\hat{\beta}(C_o) = \min \alpha \quad (58)$$

$$Subject\ to : Min\{OF\} \leq C_o \quad (59)$$

$$(1-\alpha)\tilde{P}_h^{DR} \leq P_h^{DR} \leq (1+\alpha)\tilde{P}_h^{DR} \quad (60)$$

$$\text{Eqs. } (2) - (43) \quad (61)$$

To model the decrease in the uncertainty parameter, Eq. (62) is considered which gives the minimum amount of the objective function.

$$P_h^{DR} = (1-\alpha)\tilde{P}_h^{DR} \tag{62}$$

Therefore, in the risk-taker strategy, the opportunity function will be shortened as follows:

$$\hat{\beta}(C_o) = \min \alpha \tag{63}$$

$$Subject\ to: OF \le C_o \tag{64}$$

$$P_h^{DR} = (1-\alpha)\tilde{P}_h^{DR} \tag{65}$$

$$\text{Eqs. } (2)-(43) \tag{66}$$

V. CASE STUDY

In this paper, minimizing an MG's operating cost based on IGDT based risk-constrained with taking electricity demand uncertainty is pursued. Load uncertainty is modeled via IGDT approach. As said before, MG model contains two different CHP units, PO and HO units, and ESS. TOU and RTP of DRP are proposed to decrease the MG operating costs. In this paper, it is considered that MG can exchange energy with the upstream grid according to its demand and generation.

A. INITIALIZING DATA

Figure 2 depicts the base electric and heat demand of MG in which when t = 21 and t = 4 the highest and lowest demands of electricity power are recorded. These amounts are equal to 4.65 and 1.0207, both in MW.

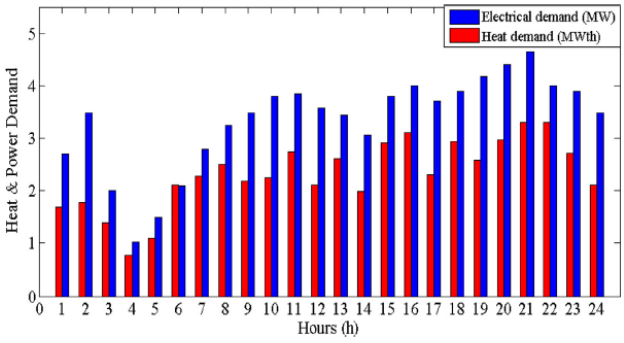

FIGURE 2. Base heat and electric power heat demands.

In Fig. 3, electric power price is shown for both DRP in which TOU prices are market price and RTP prices are obtained based on Eqs. (38)-(42). For TOU-DRP case, the highest price of electric power is experienced at h = 12 − 15 and the lowest price is occurred between at h = 22 h and h = 24. The maximum and minimum electricity price in RTP-DRP case is experienced at h = 15 − 16 and h = 4, respectively.

The information of heat buffer tank, energy storage devices, the shutdown and startup cost of units and the coefficients of cost function for FC unit are used from worthy reference [36].

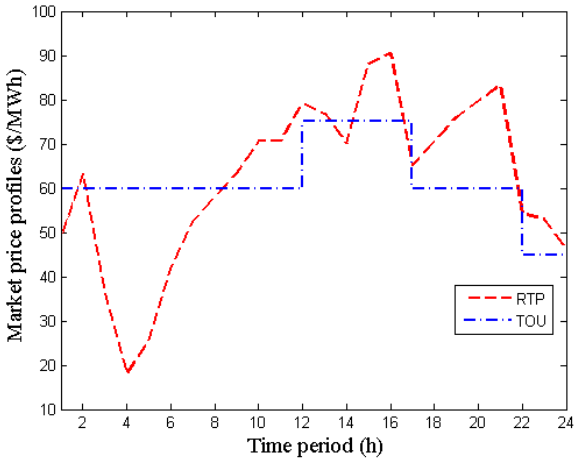

FIGURE 3. Electric power prices for each hour.

B. DETERMINISTIC CASE RESULT

By taking the degree of resistance equal to zero, the risk-neutral strategy results are obtained. In this strategy, optimal performance of MG is obtained without considering load uncertainty by minimizing (1) which is subjected to (2)-(43). MG operating cost has been reduced due to the implementation of DRPs, which the costs without DRP, with TOU-DRP and with RTP-DRP are equal to $5088 and $4959, and 4749, respectively. It can be concluded that the total cost is reduced about 2.5% and 6.6% by implementing TOU-DRP and RTP-DRP, respectively. The load change in TOU-DRP is limited to TOU price which has caused less reduction in comparison with RTP-DRP.

C. RESULT OF ROBUSTNESS FUNCTION

Maximizing Eq. (53) gives the robustness function curve which is subjected to (54)-(56). Fig. 4 illustrates robustness function (in percent) against robustness cost.

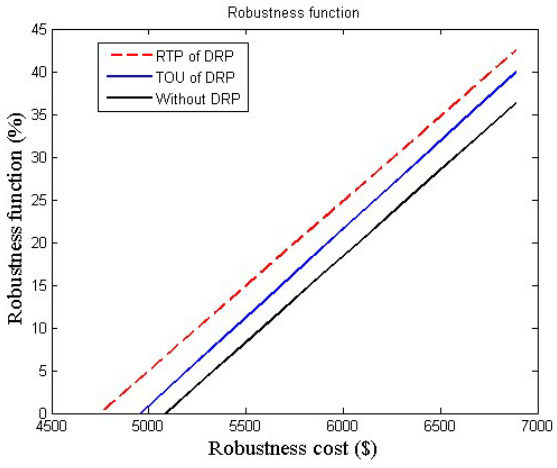

FIGURE 4. Robustness function curve.

It is clear that by increasing $\hat{\alpha}(C_r)$, the MG operating cost has increased. According to Fig. 4, by considering MG

operating cost as equal to 6000$, the MG will be robust versus load uncertainty up to 18.37%, 21.52%, and 24.82 % for without DRP, TOU-DRP, and RTP-DRP cases, respectively. Comparing these amounts show that more robust can be attained by implementing RTP-DRP in versus TOU-DRP and without DRP.

Results of the robustness function are utilized to evaluate risk-averse decision making strategies. For each of assumed cases, high operating cost indicates that the MG's strategy is highly robust and risk-averse and vice versa.

D. THE RESULT OF OPPORTUNITY FUNCTION

As discussed before, opportunity function is another function of IGDT. This function deals with uncertainty problems considering the risk-taking mode. The opportunity function is solved by minimizing (63) under constraints (64)–(66). Opportunity function curve has been illustrated in Fig. 5. In this case, the lower operating cost is desired by considering risk-taker strategy.

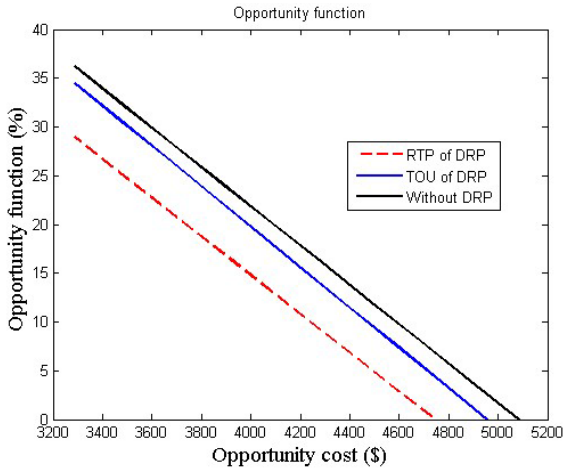

FIGURE 5. Opportunity function curve.

According to Fig. 5, MG operating cost for 28% of electric demand reduction will be equal to 3698.12$, 3605.21, and 3338.87$ for without DRP, TOU-DRP, and RTP-DRP respectively. In comparison with deterministic results, 27.31%, 27.29%, and 29.69% reduction in operating costs. In the risk-taking strategy, lower operating cost means higher risk and vice versa.

E. SCHEDULING OF COMPONENTS OF MG

In this section, the scheduling of MG's different units is reported. By assuming load uncertainty, load profile for risk-taker, risk-neutral, and risk-averse strategies have been illustrated in Fig. 6. For each strategy, three cases as without DRP, TOU-DRP, and RTP-DRP are taken into account. As was expected, the total load has been increased in risk-averse strategy while it has decreased in risk-taker strategy.

According to Figs. 3 and 6, as was expected, TOU-DRP, in all three strategies, has reduced load demand at high price

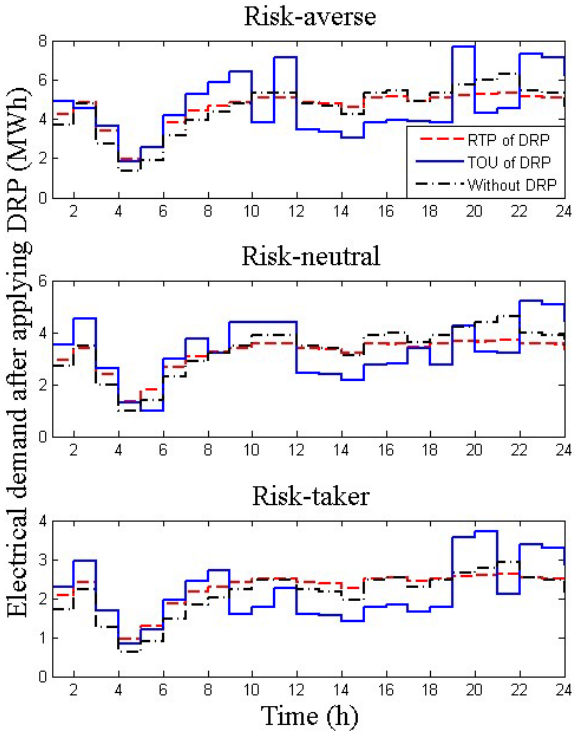

FIGURE 6. Electric load profile by considering uncertainty.

period which is experienced between h = 12 and h = 16 while it has raised load at low price times which is occurred between h = 22 and h = 24. For RTP-DRP at high price periods which are recorded at h = 12 − 16, the load has been reduced. Furthermore, low price periods have recorded at h = 4 and h = 21 − 24 which the load has been increased. On the other hand, the load-curve is more flat after applying RTP-DRP which leads better result in comparison with TOU-DRP.

MG has been assumed in the grid-connected structure which interchanges energy with the upstream-grid. The traded power between the MG and upstream-grid is depicted in Fig. 7 in which procured power is shown by positive amount while sold power is presented in negative amounts. As said before, the electrical load has been increased in risk-averse strategy. In this strategy, for all cases, more power is procured from the upstream grid in comparison with the risk-neutral case while sold power to the grid is highly reduced.

According to Fig. 6, in the risk-taker strategy, electrical demand has been reduced. Despite the risk-averse strategy, procured power from the grid has been reduced while sold power has been increased. By applying DRP, the load has reduced at peak period while has increased at off-peak period which leads to reduction in the MG's operating costs.

The generated power from the CHP units is depicted in Fig. 8. As a main internal source of demand-supply in the MG, it can be seen that aggregation of CHP's generation has not changed significantly. CHP unit's heat generation is illustrated in Fig. 9 which is used to supply heat demand in

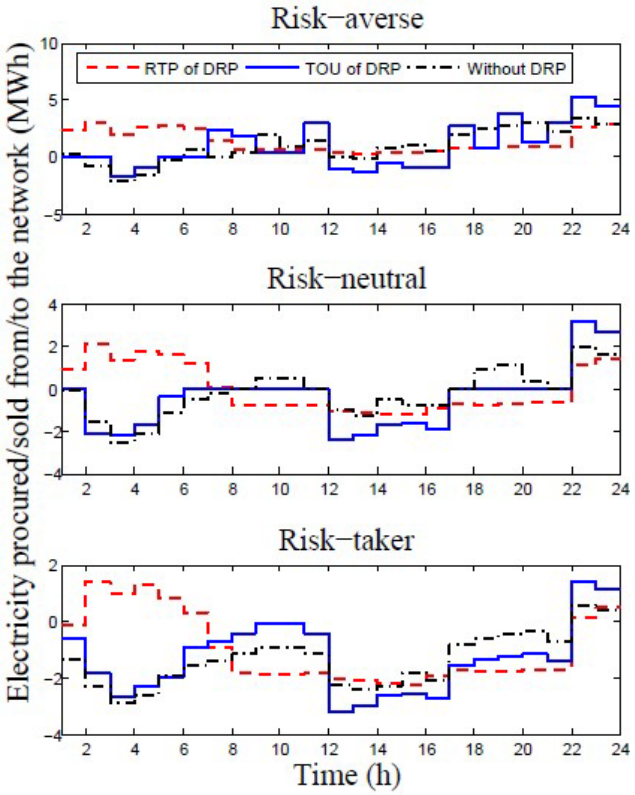

FIGURE 7. Procured/sold electric power from/to the grid.

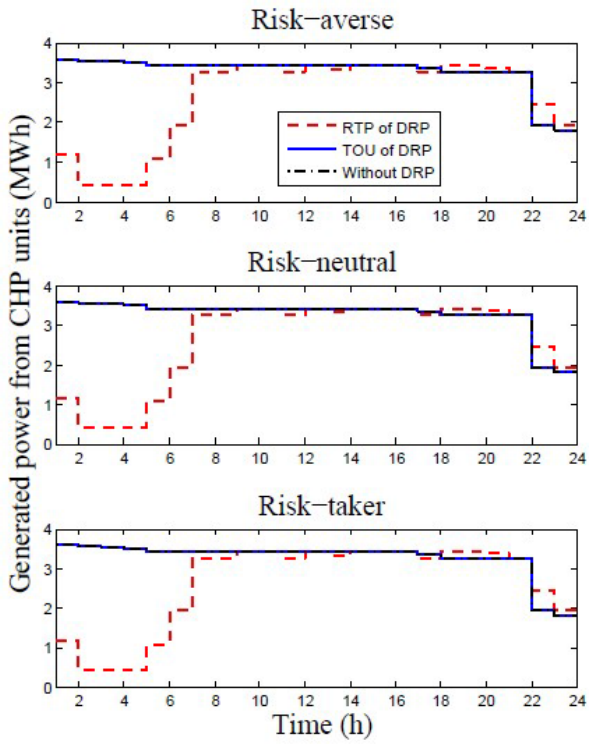

FIGURE 8. Generated power from CHP units.

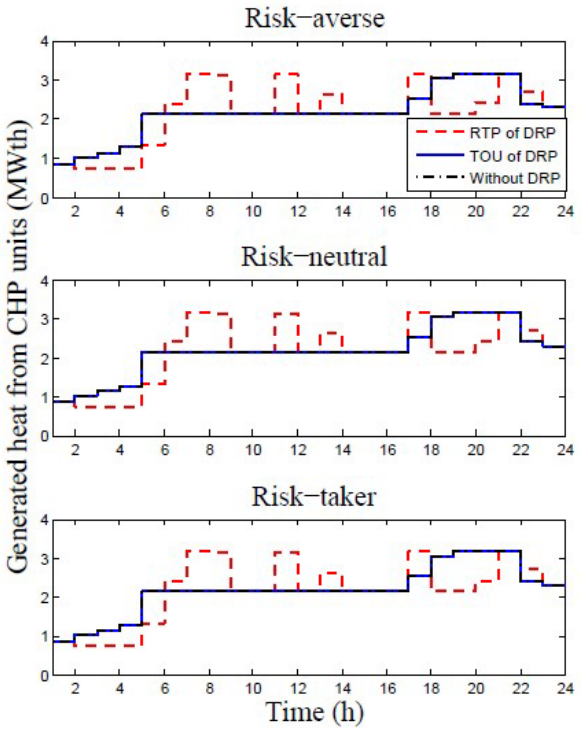

FIGURE 9. Generated heat from CHP units.

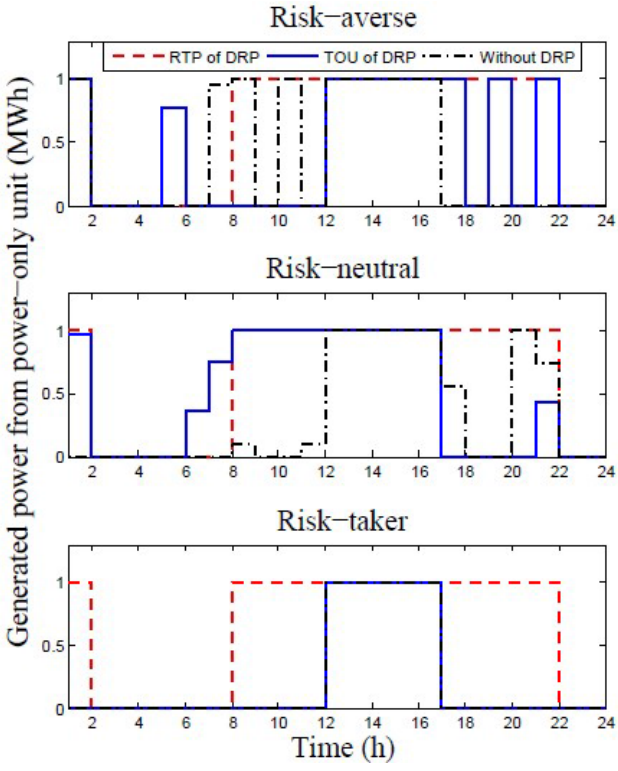

FIGURE 10. Power generation of the power-only unit.

the MG. As said before, power and heat generation of CHP units are related to each other. So, heat generation changes are very slight due to power generation's slight change.

The power only unit's power generation is illustrated in Fig. 10. In each strategy, according to load profile, generated power from this unit has changed. For example,

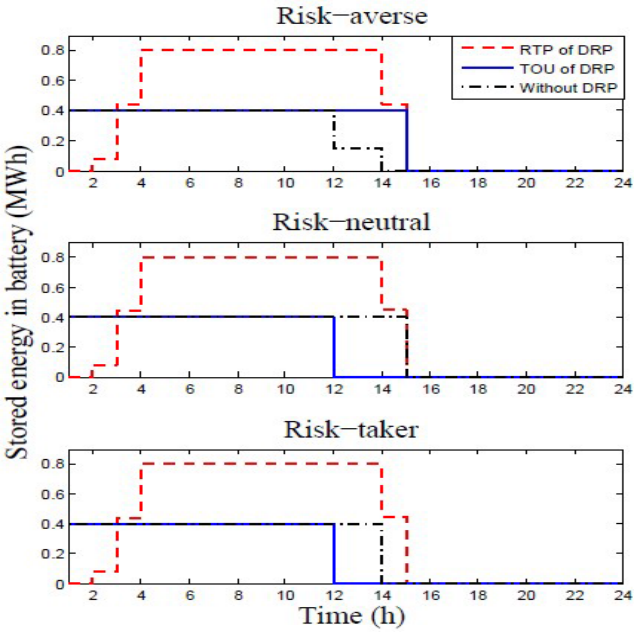

FIGURE 11. Stored energy in the storage.

by considering TOU-DRP in three strategies, due to load increment in risk-averse strategy, the power only unit's participation has increased while generated power is reduced in risk-taker strategy with respect to risk-neutral strategy.

In the MG, ESS is assumed to store excessive generated energy and inject it to the MG in needed periods. Energy stored in the battery is shown in Fig. 11. Charging and discharging of the battery is illustrated in Fig. 12. In this figure, positive amount is considered as charging power while negative amount is assumed as discharged power.

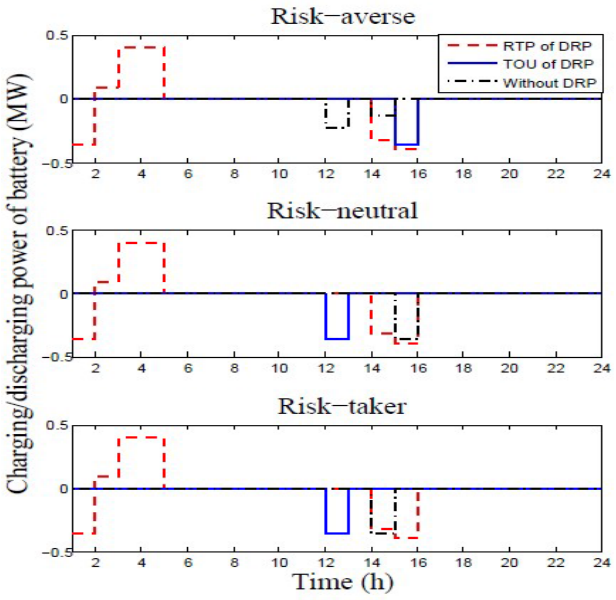

FIGURE 12. Discharging and charging power of the battery.

VI. CONCLUSION

In this work, short-time scheduling of an MG is considered in the presence of load uncertainty. Load uncertainty modeling is done by using IGDT approach. Different strategies such as risk-take, risk-neutral, and risk-averse are driven from IGDT functions in which the load profile has changed correspondingly. TOU and RTP of DRP are applied to peak load management. For each strategy, three cases as without DRP, TOU-DRT, and RTP-DRP are studied. Load uncertainty and demand response programs' effects on the load and operating cost are discussed. Results show that in deterministic mode, operating costs for without DRP, with TOU-DRP and with RTP-DRP cases are equal to \$5,088 and \$4,959, and \$4,749 respectively. This means that total operating cost is reduced about 2.5 and 6% by implementing TOU and RTP DRPs, respectively. In the robustness function curve, by considering MG operating cost as equal to \$6,000, the MG will be robust against load uncertainty up to 18.37%, 21.52%, and 24.82 % for without DRP, TOU-DRP, and RTP-DRP cases, respectively. Comparing these amounts shows that by implementing RTP-DRP better result can be attained. These results can be used to select the risk-averse decision making mode. In risk-averse strategy, the more operating cost is paid; the more robustness is attained against load uncertainty and vice versa. The risk-taker strategy is obtained by opportunity function of IGDT. Lower operating cost is desired in this strategy. MG operating cost for 28% of electric demand reduction will be equal to \$3,698.12, \$3,605.21, and \$338.87 for without DRP, TOU-DRP, and RTP-DRP cases, respectively. In comparison with deterministic results, 27.31%, 27.29%, and 29.69% reduction in operating costs. In risk taking strategy, the lower operating cost is paid, the higher risk is taken against load uncertainty and vice versa.

REFERENCES

[1] T. C. Bora, V. C. Mariani, and L. D. S. Coelho, "Multi-objective optimization of the environmental-economic dispatch with reinforcement learning based on non-dominated sorting genetic algorithm," *Appl. Thermal Eng.*, vol. 146, pp. 688–700, Jan. 2019.

[2] A. Dolatabadi and B. Mohammadi-Ivatloo, "Stochastic risk-constrained scheduling of smart energy hub in the presence of wind power and demand response," *Appl. Thermal Eng.*, vol. 123, pp. 40–49, Aug. 2017.

[3] F. Jabari, S. Nojavan, B. Mohammadi-ivatloo, H. Ghaebi, and H. Mehrjerdi, "Risk-constrained scheduling of solar stirling engine based industrial continuous heat treatment furnace," *Appl. Thermal Eng.*, vol. 128, pp. 940–955, Jan. 2018.

[4] A. Najafi-Ghalelou, S. Nojavan, and K. Zare, "Robust thermal and electrical management of smart home using information gap decision theory," *Appl. Thermal Eng.*, vol. 132, pp. 221–232, Mar. 2018.

[5] H. Yousefi, M. H. Ghodusinejad, and A. Kasaeian, "Multi-objective optimal component sizing of a hybrid ICE+PV/T driven CCHP microgrid," *Appl. Thermal Eng.*, vol. 122, pp. 126–138, Jul. 2017.

[6] S. Nojavan and H. A. Aalami, "Stochastic energy procurement of large electricity consumer considering photovoltaic, wind-turbine, micro-turbines, energy storage system in the presence of demand response program," *Energy Convers. Manage.*, vol. 103, pp. 1008–1018, Oct. 2015.

[7] W. Guo and J. Yang, "Stability performance for primary frequency regulation of hydro-turbine governing system with surge tank," *Appl. Math. Model.*, vol. 54, pp. 446–466, Feb. 2018.

[8] V. Indragandhi, R. Logesh, V. Subramaniyaswamy, V. Vijayakumar, P. Siarry, and L. Uden, "Multi-objective optimization and energy management in renewable based AC/DC microgrid," *Comput. Electr. Eng.*, vol. 70, pp. 179–198, Aug. 2018, doi: 10.1016/j.compeleceng.2018.01.023.
[9] E. Bullich-Massagué, F. Díaz-González, M. Aragüés-Peñalba, F. Girbau-Llistuella, P. Olivella-Rosell, and A. Sumper, "Microgrid clustering architectures," *Appl. Energy*, vol. 212, pp. 340–361, Feb. 2018.
[10] C. Cai, H. Liu, H. Zheng, F. Chen, L. Deng, and Q. Xu, "Microgrid multi-source coordination optimal control based on multi-scenarios analysis," *J. Eng.*, vol. 2017, no. 13, pp. 1457–1461, Jan. 2017.
[11] A. Mehdizadeh and N. Taghizadegan, "Robust optimisation approach for bidding strategy of renewable generation-based microgrid under demand side management," *IET Renew. Power Gener.*, vol. 11, no. 11, pp. 1446–1455, Sep. 2017.
[12] M. Alipour, B. Mohammadi-Ivatloo, and K. Zare, "Stochastic scheduling of renewable and CHP-based microgrids," *IEEE Trans. Ind. Informat.*, vol. 11, no. 5, pp. 1049–1058, Oct. 2015.
[13] G. Liu, M. Starke, B. Xiao, and K. Tomsovic, "Robust optimisation-based microgrid scheduling with islanding constraints," *IET Gener., Transmiss. Distrib.*, vol. 11, no. 7, pp. 1820–1828, May 2017.
[14] B. Khorramdel, H. Khorramdel, J. Aghaei, A. Heidari, and V. G. Agelidis, "Voltage security considerations in optimal operation of BEVs/PHEVs integrated microgrids," *IEEE Trans. Smart Grid*, vol. 6, no. 4, pp. 1575–1587, Jul. 2015.
[15] C. Marino, M. A. Quddus, M. Marufuzzaman, M. Cowan, and A. E. Bednar, "A chance-constrained two-stage stochastic programming model for reliable microgrid operations under power demand uncertainty," *Sustain. Energy, Grids Netw.*, vol. 13, pp. 66–77, Dec. 2017.
[16] A. Chaouachi, R. M. Kamel, R. Andoulsi, and K. Nagasaka, "Multiobjective intelligent energy management for a microgrid," *IEEE Trans. Ind. Electron.*, vol. 60, no. 4, pp. 1688–1699, Apr. 2013.
[17] M. Di Somma, B. Yan, N. Bianco, G. Graditi, P. B. Luh, L. Mongibello, and V. Naso, "Multi-objective design optimization of distributed energy systems through cost and exergy assessments," *Appl. Energy*, vol. 204, pp. 1299–1316, Oct. 2017.
[18] Z. Li and Y. Xu, "Optimal coordinated energy dispatch of a multi-energy microgrid in grid-connected and islanded modes," *Appl. Energy*, vol. 210, pp. 974–986, Jan. 2018.
[19] A. Maulik and D. Das, "Optimal operation of microgrid using four different optimization techniques," *Sustain. Energy Technol. Assessments*, vol. 21, pp. 100–120, Jun. 2017.
[20] X. P. Chen, N. Hewitt, Z. T. Li, Q. M. Wu, X. Yuan, and T. Roskilly, "Dynamic programming for optimal operation of a biofuel micro CHP-HES system," *Appl. Energy*, vol. 208, pp. 132–141, Dec. 2017.
[21] M. Nemati, M. Braun, and S. Tenbohlen, "Optimization of unit commitment and economic dispatch in microgrids based on genetic algorithm and mixed integer linear programming," *Appl. Energy*, vol. 210, pp. 944–963, Jan. 2018.
[22] M. Alipour, K. Zare, and B. Mohammadi-Ivatloo, "Short-term scheduling of combined heat and power generation units in the presence of demand response programs," *Energy*, vol. 71, pp. 289–301, Jul. 2014.
[23] B. Mohammadi-Ivatloo, M. Moradi-Dalvand, and A. Rabiee, "Combined heat and power economic dispatch problem solution using particle swarm optimization with time varying acceleration coefficients," *Electr. Power Syst. Res.*, vol. 95, pp. 9–18, Feb. 2013.
[24] M. Elsied, A. Oukaour, H. Gualous, and R. Hassan, "Energy management and optimization in microgrid system based on green energy," *Energy*, vol. 84, pp. 139–151, May 2015.
[25] C. Wang, Y. Liu, X. Li, L. Guo, L. Qiao, and H. Lu, "Energy management system for stand-alone diesel-wind-biomass microgrid with energy storage system," *Energy*, vol. 97, pp. 90–104, Feb. 2016.
[26] S. Nojavan, H. Ghesmati, and K. Zare, "Robust optimal offering strategy of large consumer using IGDT considering demand response programs," *Electr. Power Syst. Res.*, vol. 130, pp. 46–58, Jan. 2016.
[27] M. Jin, W. Feng, C. Marnay, and C. Spanos, "Microgrid to enable optimal distributed energy retail and end-user demand response," *Appl. Energy*, vol. 210, pp. 1321–1335, Jan. 2018.
[28] L. Montuori, M. Alcázar-Ortega, C. Álvarez-Bel, and A. Domijan, "Integration of renewable energy in microgrids coordinated with demand response resources: Economic evaluation of a biomass gasification plant by Homer simulator," *Appl. Energy*, vol. 132, pp. 15–22, Nov. 2014.
[29] G. S. Piperagkas, A. G. Anastasiadis, and N. D. Hatziargyriou, "Stochastic PSO-based heat and power dispatch under environmental constraints incorporating CHP and wind power units," *Electric Power Syst. Res.*, vol. 81, no. 1, pp. 209–218, Jan. 2011.
[30] T. Niknam, A. Kavousifard, S. Tabatabaei, and J. Aghaei, "Optimal operation management of fuel cell/wind/photovoltaic power sources connected to distribution networks," *J. Power Sources*, vol. 196, no. 20, pp. 8881–8896, Oct. 2011.
[31] M. Shahverdi and S. M. Moghaddas-Tafreshi, "Operation optimization of fuel cell power plant with new method in thermal recovery using particle swarm algorithm," in *Proc. 3rd Int. Conf. Electric Utility Deregulation Restructuring Power Technol.*, Apr. 2008, pp. 2542–2547.
[32] S. Nojavan, K. Zare, and B. Mohammadi-Ivatloo, "Optimal stochastic energy management of retailer based on selling price determination under smart grid environment in the presence of demand response program," *Appl. Energy*, vol. 187, pp. 449–464, Feb. 2017.
[33] S. Nojavan, H. Qesmati, K. Zare, and H. Seyyedi, "Large consumer electricity acquisition considering time-of-use rates demand response programs," *Arabian J. Sci. Eng.*, vol. 39, no. 12, pp. 8913–8923, Dec. 2014.
[34] S. Nojavan, K. Zare, and M. R. Feyzi, "Optimal bidding strategy of generation station in power market using information gap decision theory (IGDT)," *Electric Power Syst. Res.*, vol. 96, pp. 56–63, Mar. 2013.
[35] S. Nojavan, H. Pashaei-Didani, K. Saberi, and K. Zare, "Risk assessment in a central concentrating solar power plant," *Sol. Energy*, vol. 180, pp. 293–300, Mar. 2019.
[36] M. Nazari-Heris, S. Abapour, and B. Mohammadi-Ivatloo, "Optimal economic dispatch of FC-CHP based heat and power micro-grids," *Appl. Thermal Eng.*, vol. 114, pp. 756–769, Mar. 2017.

SAYYAD NOJAVAN received the B.Sc., M.Sc., and Ph.D. degrees in electrical power engineering from the University of Tabriz, Tabriz, Iran, in 2010, 2012, and 2017, respectively. He was a Postdoctoral Researcher with the Faculty of Electrical and Computer Engineering, University of Tabriz, from September 2017 to September 2018. He is currently an Assistant Professor with the Department of Electrical Engineering, University of Bonab, Bonab, Iran. His research areas include distribution networks operation, power system operation and economics, electricity market, demand response applications, hybrid energy systems, uncertainty modeling, and risk management. He has also edited several books in the electrical and energy fields in Springer and Elsevier publications.

KITTISAK JERMSITTIPARSERT received the Ph.D. degree in social sciences from Kasetsart University, Thailand. He is currently a Researcher with the Chulalongkorn University Social Research Institute, a part-time Researcher with Ton Duc Thang University, and the Secretary General of the Political Science Association, Kasetsart University. His areas of expertise are politics, public policy, business, development, and energy management.